

This is the accepted manuscript made available via CHORUS. The article has been published as:

## Viscosity of fused silica and thermal noise from the standard linear solid model

N. M. Kondratiev and M. L. Gorodetsky

Phys. Rev. D **94**, 081102 — Published 27 October 2016

DOI: [10.1103/PhysRevD.94.081102](https://doi.org/10.1103/PhysRevD.94.081102)

# Viscosity of fused silica and thermal noise from SLS model

N.M. Kondratiev

*Russian Quantum Center, Skolkovo 143025, Russia*

M. L. Gorodetsky\*

*Russian Quantum Center, Skolkovo 143025, Russia and*

*Faculty of Physics, M.V. Lomonosov Moscow State University, 119991 Moscow, Russia*

The Fluctuation-Dissipation Theorem states that each source of dissipation yields corresponding fluctuations. The most obvious source of dissipation in liquids is viscosity – internal friction between layers of matter. However this property also exists in solid materials in glass state – amorphous substance that couldn't become a crystal due to high viscosity. Fused silica is a low-loss glass material used in many interferometric applications demanding high stability as Fabry-Perot etalons and gravitational wave detector mirrors and suspensions. Very high viscosity (ranged from  $10^{17}$  to  $10^{40}$  Pa s in literature) can be the source of additional noise, and influence performance of such devices. We show that fused silica may be described with the Standard Linear Solid model of viscoelasticity and present a method to estimate this type of noise.

PACS numbers: 04.80.Nn, 42.79.Wc, 07.60.Ly, 05.40.Ca

## I. INTRODUCTION

For modern high precision measurements any source of noise can be critical. The LIGO project [1] that resulted in first direct observation of gravitational waves [2] has to account many fundamental sources of fluctuations. The Brownian noise coming from chaotic thermal motion of particles is one of the enemies. Thermal noise in coatings, substrates and suspensions of the interferometer's mirrors results in fluctuations of their surfaces which add a phase noise to the signal [3, 4]. A lot of other processes can degrade the sensitivity of the device [5, 6].

The common way to calculate thermal noises is a Fluctuation- Dissipation Theorem. It states that any dissipation in a system results in added fluctuations. The theory gives the spectral density of surface fluctuations in mirrors of the LIGO antennae in the form [3]:

$$S(\omega) = \frac{4k_B T}{\omega} \text{Im}[\alpha_s + \alpha_j^c + \alpha_j^s], \quad (\text{I.1})$$

where  $\omega$  is the frequency,  $k_B$  is the Boltzmann's constant and  $T$  is the temperature,  $\alpha_s$  is dynamic permittivity of the substrate,  $\alpha_j^c$  and  $\alpha_j^s$  are coating and coating induced substrate dynamic permittivities. In [3, 7, 8] those values were found to be

$$\alpha_s = \frac{1}{\sqrt{\pi}w} \frac{1 - \nu_s^2}{Y_s}, \quad (\text{I.2})$$

$$\alpha_j^c = \sum_j \frac{\beta_j d_j}{\pi w^2} \frac{(1 + \nu_j)(1 - 2\nu_j)}{Y_j(1 - \nu_j)}, \quad (\text{I.3})$$

$$\alpha_j^s = \sum_j \frac{d_j}{\pi w^2} \frac{Y_j}{1 - \nu_j^2} \frac{(1 + \nu_s)^2(1 - 2\nu_s)^2}{Y_s^2}, \quad (\text{I.4})$$

where  $w$  is the Gaussian beam radius on the mirror,  $Y_s$  and  $\nu_s$  are Young's modulus and Poisson coefficient of the substrate,  $Y_j$  and  $\nu_j$  are the parameters of  $j$ -th coating layer,  $d_j$  and  $\beta_j$  are thickness and interference coefficient of  $j$ -th coating layer. The dissipation is then introduced empirically in the form of the loss angle  $Y \rightarrow Y(1 - i\phi)$ .

There are several models that try to describe this loss angle theoretically [9, 10] and phenomenologically [11]. Viscosity is one of the sources of dissipation. In the following section we show that viscosity can be introduced into equations in the same way, providing a new type of noise.

## II. MODEL OF VISCOSITY

In hydrodynamics the viscosity can be introduced into Navier-Stokes equation through the viscose stress tensor  $\sigma_{ik}^v$ :

$$\sigma_{ik}^v = \eta \left[ \frac{\partial v_i}{\partial x_k} + \frac{\partial v_k}{\partial x_i} - \frac{2}{3} \delta_{ik} \frac{\partial v_l}{\partial x_l} \right] + \zeta \delta_{ik} \frac{\partial v_l}{\partial x_l}, \quad (\text{II.1})$$

where  $\eta$  is the shear viscosity,  $\zeta$  is the volume viscosity and  $\vec{v}$  is the velocity of the particles. Combined with tensor Hooke's law it gives the Kelvin-Voigt model for viscoelastic materials, which works well for modeling creep in solid materials [12]. This model was also successfully used to explain experimental data in [13]. However, this model does not give correct results for ultrasonic losses in our case of high-viscosity limit as in spectral representation it corresponds to complex substitution of shear and bulk moduli

$$K \rightarrow K + i\omega\zeta, \quad (\text{II.2})$$

$$G \rightarrow G + i\omega\eta. \quad (\text{II.3})$$

It can be shown that this results in unrealistically high noise and even leads to wrong dispersion relation for

---

\* mg@rqc.ru

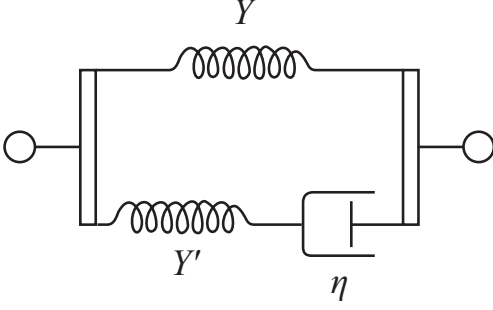


FIG. 1. “Elementary cell” of the SLS model.

sound waves. There is another viscosity model, called Maxwell model which is usually used for glasses [14]. However, this model does not lead to exponential matter flow rate measured in [15] and allows infinite motion that was not observed in experiment [16]. That is why we use

$$\begin{aligned} \left(1 + \frac{G}{G'}\right) \dot{\varepsilon} + \frac{1}{3} \left(\frac{K}{K'} - \frac{G}{G'}\right) \text{tr}(\dot{\varepsilon}) + \frac{G}{\eta} \varepsilon + \frac{1}{3} \left(\frac{K}{\zeta} - \frac{G}{\eta}\right) \text{tr}(\varepsilon) = \\ \frac{\dot{\sigma}}{2G'} + \frac{1}{3} \left(\frac{1}{3K'} - \frac{1}{2G'}\right) \text{tr}(\dot{\sigma}) + \frac{\sigma}{2\eta} + \frac{1}{3} \left(\frac{1}{3\zeta} - \frac{1}{2\eta}\right) \text{tr}(\sigma) \end{aligned} \quad (\text{II.4})$$

where indices  $i$  and  $j$  in stress  $\sigma$  and strain  $\varepsilon$  tensor notation, so as delta functions  $\delta_{ij}$  in front of trace are omitted. Having dynamic moduli  $G', K' \rightarrow \infty$  we arrive at the Kelvin-Voigt. Having  $K, G \rightarrow 0$  (long-term spring removed), we come to Maxwell model. Finally, in high viscosity limit ( $\eta, \zeta \rightarrow \infty$ ) the problem reduces to general static problem with “quasi-static” moduli  $G_0 = G + G'$  and  $K_0 = K + K'$  that describe both high-frequency experiments and static load experiments held at time scales less than several years.

Taking spectral representation of (II.4) we can get the following complex substitution for shear and bulk moduli with which we can introduce viscous losses:

$$K \rightarrow K + \frac{i\omega\zeta K'}{K' + i\omega\zeta}, \quad (\text{II.5})$$

$$G \rightarrow G + \frac{i\omega\eta G'}{G' + i\omega\eta}. \quad (\text{II.6})$$

Unfortunately, the parameters of the model  $G', K', G, K$  as well as viscous parameters  $\eta, \zeta$  at room temperatures are difficult to measure.

#### A. Standard Linear Solid parameters

To estimate the SLS parameters of fused silica a series of recent results [13, 15, 16] may be used. In those works

a more general Standard Linear Solid model (SLS) for viscoelastic materials [17].

The SLS model can be illustrated with the spring diagram, shown on figure 1. This “elementary cell” consists of a first (static or long-term) spring  $Y$  with shear and bulk moduli  $G$  and  $K$ , second (dynamic) spring  $Y'$  with parameters  $G'$  and  $K'$ , and a dashpot with shear and bulk (volumetric) viscosity  $\eta$  and  $\zeta$ . The first spring governs the static behavior of the system while the higher frequency motion uses both. Here we should note, however, that for ultra high viscosities of glasses all “static” load experiments are too fast for the second spring to relax (unless they are made at timescale of years). In this way both in measurements of speed of sound and in static load experiments only the sum of the above introduced moduli is observed. This can be also shown directly using the model master equations (II.4), tending viscosities to infinity.

The master equation for the tensor stress-strain relationship in Standard Linear Solid model is

a flow of fused silica plates during decades under their own weight was studied. We propose to reconsider these results in the view of SLS model.

Assuming that time dependence of the fields can be separated from coordinate part so that  $\hat{\varepsilon}(\vec{r}, t) = \hat{\varepsilon}(\vec{r})T(t)$  and  $\hat{\sigma}(\vec{r}, t) = \hat{\sigma}(\vec{r})T_s(t)$ , and using (II.4) we obtain:

$$\frac{\sigma_{\mu>3}(\vec{r})}{\varepsilon_{\mu>3}(\vec{r})} = \frac{(1 + G/G')\dot{T} + GT/\eta}{\dot{T}_s/(2G') + T_s/(2\eta)} = C_G, \quad (\text{II.7})$$

$$\frac{\text{tr}(\sigma(\vec{r}))}{\text{tr}(\varepsilon(\vec{r}))} = \frac{(1 + K/K')\dot{T} + KT/\zeta}{\dot{T}_s/(3K') + T_s/(3\zeta)} = C_K, \quad (\text{II.8})$$

where  $\mu > 3$  means non-diagonal terms (Voigt notation). The direct expressions for stress tensor diagonal can also be obtained:

$$\frac{\sigma_{\mu\leq 3}(\vec{r})}{\varepsilon_{\mu\leq 3}(\vec{r})} = C_G + \frac{1}{3}(C_K - C_G) \frac{\text{tr}(\varepsilon(\vec{r}))}{\varepsilon_{\mu\leq 3}(\vec{r})}. \quad (\text{II.9})$$

The form of the relations (II.7)-(II.9) suggests that there are probably two different oscillatory behaviors (e.g. time dependences) for diagonal (related to volumetric) and non-diagonal (related to shear motion) terms of the tensors. In this way the displacement vector may be decomposed in two parts as  $\vec{u}(\vec{r}, t) = \vec{u}_K(\vec{r})T_K(t) + \vec{u}_G(\vec{r})T_G(t)$ . So for stress tensor we also can write  $\hat{\sigma}(\vec{r}, t) = \hat{\sigma}_K(\vec{u}_K)T_{s_K}(t) + \hat{\sigma}_G(\vec{u}_G)T_{s_G}(t)$ . Note that  $\sigma_G$  and  $\sigma_K$  act like linear differential operators.

The equation of elastic motion can be written as following [18]:

$$\rho \ddot{\vec{u}} = -\rho g + \text{div } \hat{\sigma}, \quad (\text{II.10})$$

where  $\rho$  is density,  $g$  is gravity acceleration, and  $\text{div } \hat{\sigma} = \frac{\partial \sigma_{ik}}{\partial x_k}$  in Cartesian system of coordinates. Substituting the above suggested decomposition into homogeneous equations we can see that due to linearity we can treat equations for  $\vec{u}_K$  and  $\vec{u}_G$  separately. Furthermore the equations are of the same form with respect to the partial index ( $K$  or  $G$ ). The displacements should be matched to satisfy the boundary conditions. The solution can be introduced in the form of the sum of a particular solution of full equation and a combination of solutions of homogeneous equations. Nontrivial homogeneous equations of motion for cylindrical symmetry ( $u_\varphi = 0$  and  $\frac{\partial}{\partial \varphi} = 0$ ), omitting the part index can be written as follows:

$$\rho \ddot{T} u_r = T_s \left( \frac{1}{r} \frac{\partial}{\partial r} (r \sigma_r) + \frac{\partial}{\partial z} \sigma_5 \right), \quad (\text{II.11})$$

$$\rho \ddot{T} u_z = T_s \left( \frac{1}{r} \frac{\partial}{\partial r} (r \sigma_5) + \frac{\partial}{\partial z} \sigma_z \right). \quad (\text{II.12})$$

Now dividing the equations over  $T_s$  we collect all time-dependent variables on the right and coordinate-dependent on the left, thus performing coordinate separation. So we get  $\ddot{T}/T_s = k^2$ , where  $k^2$  is the separation parameter in units of  $1/(\text{Pa}^{1/2} \text{ s})$ . This constant enumerates the solutions of homogeneous equation and is to be summed over in attempt to satisfy the boundary conditions. It is shown further that this value is not needed for the determination of time constant. Combining this result with (II.7) and (II.8) we find the temporal parts of equations in the form

$$-k^2 \left( (1 + G/G') \dot{T} + \frac{G}{\eta} T \right) = \frac{1}{2G'} \ddot{T} + \frac{1}{2\eta} \dot{T}. \quad (\text{II.13})$$

The corresponding equation and solution for volumetric part is obtained by changing  $G \rightarrow K$ ,  $\eta \rightarrow \zeta$  and  $2 \rightarrow 3$ . This equation for high viscosity approximation provides three time constants:

$$\gamma_0 = -\frac{GG'}{\eta(G + G')}, \quad (\text{II.14})$$

$$\gamma_{\pm} = -\frac{G'^2}{2\eta(G + G')} \pm ik\sqrt{G + G'}. \quad (\text{II.15})$$

This results in a solution in the form of damped ( $e^{\text{Re}\gamma_{\pm}t}$ ) oscillations with frequencies  $\text{Im}\gamma_{\pm}$ , near momentary equilibrium, exponentially ( $e^{\gamma_0 t}$ ) approaching the final stationary displacement  $U_0$ . Note that  $\gamma_0$  is independent of  $k$  and thus on the whole coordinate part solution, factorizing overall exponential decay tendency. In this way we obtain the exponential tendency function  $U_0(1 - \exp(\gamma_0(t - t_0)))$  used in [15] to approximate the

experimental data. Although it can be shown numerically that there is more energy in volume part of deformations, we assume that this exponential damping is related mostly to shear process. The observable is the  $z$ -displacement in the mirror's center which can be estimated as  $\int_{\text{thickness}} \varepsilon_{zz} dz + \int_{\text{radius}} \varepsilon_{rz} dr$ , thus the shear part scales with the disc radius and prevails.

The parameters  $U_0$  and  $\gamma_0^{-1}$  of exponential approximation are badly determined (40% and 111% of relative variance for 95% confidence). So we use estimations obtained for the last two plates [13]. It was shown that their relaxation has already finished (a year shift was less than the accuracy limit of 0.5 nm), allowing the authors to extract the parameters with 10% accuracy.

We can get an estimate for  $U_0$  from stationary consideration that obviously coincides with the common one [19, 20]:

$$U_0 = \frac{g\rho R^2}{16Yh^2} (3(5R^2 + 4h^2) - 4(3R^2 - h^2)\nu - 3R^2\nu^2), \quad (\text{II.16})$$

where  $Y = \frac{9KG}{3K+G}$  is Young modulus,  $\nu = \frac{3K-2G}{2(3K+G)}$  is Poisson ratio,  $R$  is plate radius,  $h$  is its thickness and  $\rho$  is density. To complete the system of equations we use expressions for longitudinal and transversal speed of sound, modified according to the SLS model (II.5), (II.6) at high frequency and viscosity limit:

$$v_l^2 \approx \frac{3(K + K') + 4(G + G')}{3\rho} \quad (\text{II.17})$$

$$v_t^2 \approx \frac{G + G'}{\rho} \quad (\text{II.18})$$

In addition we make an assumption that the Poisson ratio for static parameters should be of the same order as that for quasi-static one. Being small this should be suitable for our estimations

Used	values	Estimated	values
$U_0$	35 ,nm	$K$	8.7 GPa
$\nu_0$	0.17	$G$	7.3 GPa
$c_t$	3764 m/s	$G'$	23.8 GPa
$\gamma_0^{-1}$	12 years	$\eta$	$2.1 \times 10^{18} \text{ Pa}\cdot\text{s}$

TABLE I. Material parameters obtained from literature and estimated.

The results are summarized in table I. The estimated viscosity is 10 times higher than that obtained in original paper [13]. Nevertheless it is still much less than extrapolation values following from high-temperature measurements.

### III. VISCOSITY NOISE

We can now use permittivities (I.2)-(I.4) with the substitution (II.5)-(II.6) to calculate the noises.

$$S_s = \frac{4k_B T}{\omega^2} \frac{1}{4\sqrt{\pi}w(v_l^2 - v_t^2)^2 v_t^4 \rho^2} \left( v_t^4 \frac{K'^2}{\zeta} + (3v_l^4 - 6v_l^2 v_t^2 + 4v_t^4) \frac{G'^2}{3\eta} \right), \quad (\text{III.1})$$

$$S_j^c = \frac{4k_B T}{\omega^2} \sum_j \frac{|\beta_j|^2 d_j}{\pi w^2} \frac{1}{v_{t_j}^4 \rho_j^2} \left( \frac{K_j'^2}{\zeta_j} + \frac{4G_j'^2}{3\eta_j} \right), \quad (\text{III.2})$$

$$S_j^s = \frac{4k_B T}{\omega^2} \sum_j \frac{d_j}{\pi w^2} \frac{1}{(v_l^2 - v_t^2)^2 v_{t_j}^4 \rho^2} \left( 2v_{l_j}^2 v_{t_j}^2 \frac{\rho_j(v_{l_j}^2 - v_{t_j}^2)}{\rho(v_l^2 - v_t^2)} \left( \frac{K'^2}{\zeta} + \frac{G'^2}{3\eta} \right) - \left( v_{t_j}^4 \frac{K_j'^2}{\zeta_j} + (3v_{l_j}^4 - 6v_{l_j}^2 v_{t_j}^2 + 4v_{t_j}^4) \frac{G_j'^2}{3\eta_j} \right) \right). \quad (\text{III.3})$$

Here  $v_l^2$  and  $v_t^2$  – longitude and transverse wave velocities of the substrate and  $j$ -th layer,  $G'$   $K'$  – short time shear and bulk moduli of substrate and  $j$ -th layer,  $\eta$   $\zeta$  – shear and bulk viscosity of substrate and  $j$ -th layer,  $\rho$  – materials' densities.

Layer	$\nu$	$n$	$Y$ GPa	$\phi$
s	0.17	1.45	72	$7.6 \times 10^{-12} f^{0.77}$
l	0.17	1.45	72	$0.4 \times 10^{-4}$
h	0.23	2.06	140	$2.3 \times 10^{-4}$

TABLE II. Substrate (s), high-refractive (h) and low refractive (l) layer parameters, used for calculation. Other constants are  $\lambda = 1.064$  mkm;  $w = 0.06$  m;  $T = 290$  K.

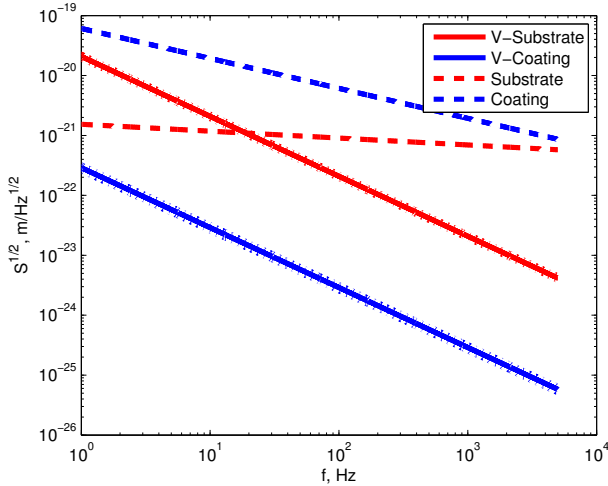


FIG. 2. Brownian noises from substrate and coating (dashed lines) for parameters from table II according to [21] with viscosity noises (solid lines). The error estimation is 15% (dots).

We use mirror parameters from [21], given in Table II. Here “l” stands for low refraction material (silica), “h” stands for high refraction material (tantala) and “s” for substrate (high-quality silica).  $Y$  and  $\sigma$  are Young modulus and Poisson ratio of the layers (used to estimate Brownian noises),  $n$  goes for refraction indices,  $\phi$  goes for

loss angles,  $\lambda$  is laser wavelength,  $w$  is the laser beam spot radius ( $e^{-2}$  power) and  $T$  is temperature.

The numerical estimates of silica part together with the standard Brownian noise is shown on Fig. 2. The coating part appears to be by several orders lower than viscosity substrate noise due to it's small thickness. It can be neglected until tantala has its viscosity at least 5 orders smaller than silica does (see fig.3).

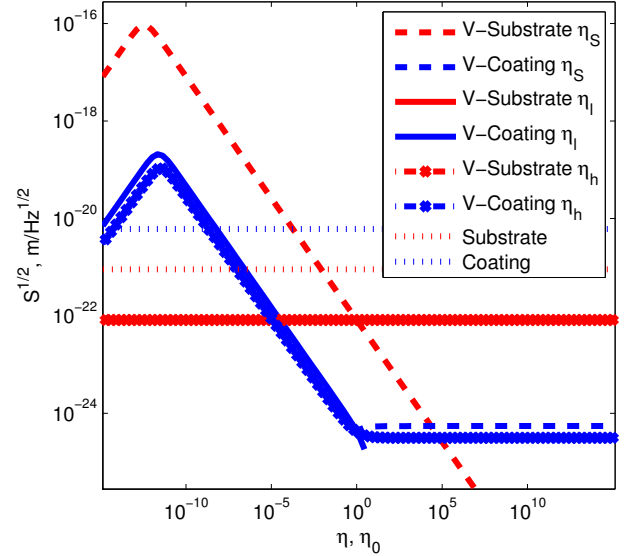


FIG. 3. Brownian and viscosity noises at 100 Hz depending on the viscosity of the substrate  $\eta_s$ , silica layer  $\eta_l$  or tantala layer  $\eta_h$  in units of  $\eta_0 = 2.1 \times 10^{18}$  Pa.s. The rest of the viscosities were taken equal to  $\eta_0$  for each curve.

#### IV. CONCLUSION

The viscosity of fused silica can be the source of additional noise in LIGO antennae exceeding the substrate Brownian noise at frequencies below 19 Hz. However, if we use the viscosity value as calculated in [16] this point moves close to 100 Hz – the maximum of LIGO sensitivity. Furthermore, the whole volumetric part of the

noise is unknown due to absence of appropriate material parameters data.

Another uncertainty is attributed to viscosity in mirror's coating which is totally unknown. Remembering that regular mechanical coating losses are three orders of magnitude higher than in bulk material making coating Brownian noise the limiting factor of the LIGO detector, viscosity in stressed coating may suggest surprises. Note that the less is the viscosity, the higher is the noise. We also note that temperature reduction may be an efficient way to reduce the viscosity noise increasing viscosity itself. Nevertheless, the coating Brownian noise still prevails remaining the limiting factor for LIGO interfer-

ometers for now.

We also conclude that fused silica can be described by the Maxwell model of viscosity for times, smaller than 12 years from the start of relaxation, while the SLS model should be used otherwise.

## ACKNOWLEDGMENTS

The authors acknowledge support from the Russian Foundation for Basic Research (Grant No. 14-02-00399A) and National Science Foundation (Grant No. PHY-1305863)

- 
- [1] B. P. Abbott et. al. (LIGO Scientific Collaboration and Virgo Collaboration), Reports on Progress in Physics **72**, 076901 (2009).
  - [2] B. P. Abbott et. al. (LIGO Scientific Collaboration and Virgo Collaboration), Physical Review Letters **116**, 241102 (2016).
  - [3] G. M. Harry, A. M. Gretarsson, P. R. Saulson, S. E. Kittelberger, S. D. Penn, W. J. Startin, S. Rowan, M. M. Fejer, D. R. M. Crooks, G. Cagnoli, J. Hough, and N. Nakagawa, Classical and Quantum Gravity **19**, 897 (2002).
  - [4] G. M. Harry, H. Armandula, E. Black, D. R. M. Crooks, G. Cagnoli, J. Hough, P. Murray, S. Reid, S. Rowan, P. Sneddon, M. M. Fejer, R. Route, and S. D. Penn, Appl. Opt. **45**, 1569 (2006).
  - [5] M. L. Gorodetsky, Physics Letters A **372**, 6813 (2008).
  - [6] M. Evans, S. Ballmer, M. Fejer, P. Fritschel, G. Harry, and G. Ogin, Phys. Rev. D **78**, 102003 (2008).
  - [7] A. Gurkovsky and S. Vyatchanin, Physics Letters A **374**, 3267 (2010).
  - [8] N. M. Kondratiev, A. G. Gurkovsky, and M. L. Gorodetsky, Phys. Rev. D **84**, 022001 (2011).
  - [9] R. Vacher, E. Courtens, and M. Foret, Phys. Rev. B **72**, 214205 (2005).
  - [10] A. E. Duwel, J. Lozow, C. J. Fisher, T. Phillips, R. H. Olsson, and M. Weinberg, Proc. SPIE **8031**, 80311C (2011).
  - [11] S. D. Penn, A. Ageev, D. Busby, G. M. Harry, A. M. Gretarsson, K. Numata, and P. Willems, Physics Letters A **352**, 3 (2006).
  - [12] R. Tanner, *Engineering Rheology*, Oxford engineering science series (Oxford University Press, 2000).
  - [13] M. Vannoni, A. Sordini, and G. Molesini, The European Physical Journal E **34**, 1 (2011).
  - [14] F. Richter, *Upsetting and Viscoelasticity of Vitreous SiO<sub>2</sub>: Experiments, Interpretation and Simulation*, Ph.D. thesis, Technische Universitat Berlin (2006).
  - [15] M. Vannoni, A. Sordini, and G. Molesini, Opt. Express **18**, 5114 (2010).
  - [16] M. Vannoni, A. Sordini, and G. Molesini, Proc. SPIE **8169**, 816906 (2011).
  - [17] Y. de Haan and G. Sluimer, Heron **46**, 49 (2001).
  - [18] L. Landau, L. Pitaevskii, A. Kosevich, and E. Livshitz, *Theory of Elasticity*, Course of theoretical physics, Vol. 7 (Elsevier Science, 2012).
  - [19] W. Emerson, J. Res. Bur. Stand. **49**, 241 (2007).
  - [20] S. Timoshenko and S. Woinowsky-Krieger, *Theory of plates and shells*, McGraw-Hill classic textbook reissue series (McGraw-Hill, 1959).
  - [21] The LIGO Scientific Collaboration, "Gravitational wave interferometer noise calculator (GWINC)," <https://awiki.ligo-wa.caltech.edu/aLIGO/GWINC>.